A NUMERICAL STUDY OF THE EFFECTS OF COLD WATER INJECTION ON THE PRESSURE TRANSIENT RESPONSE AND INJECTION CAPACITY OF GEOTHERMAL WELLS

Jefferson D. Villacorte[1], and Michael J. O' Sullivan[2]

[1]Energy Development Corporation, 38th Floor One Corporate Centre Building, Julia Vargas Corner Meralco Avenue, Ortigas Center, 1605 Pasig City, Philippines
[2]Department of Engineering Science, University of Auckland, Auckland 1142 New Zealand

villacorte.jd@energy.com.ph, m.osullivan@auckland.ac.nz

Keywords: cold water injection, pressure transient, simulation, well-testing analysis, inverse modeling

ABSTRACT

This study examines how the formation permeability varies during injection/fall-off tests of geothermal wells and thus how injection of cold water affects the injectivity of the well thereafter.

Pressure data measured during cold water injection tests were analyzed and simulations were conducted to obtain a match to the data. In some cases the data were divided into separate sections during different rates of injection and during the fall-off phases. Simulations of the tests were carried out with commercially available well testing software (SAPHIR and AWTAS), and established multiphase, multi-component numerical codes (TOUGH2 and FEHM). Various model configurations were defined and several well/rock parameter combinations were specified to achieve improvement of the fit to the transient data. Inverse modeling was performed with PEST and iTOUGH to achieve further improvement of the correspondence between actual and simulated values.

1. INTRODUCTION

Cold water injection tests are often performed on geothermal wells, usually for one of the following reasons: (i) to obtain pressure transient data from which the reservoir transmissivity and skin factor of the well can be calculated, (ii) to stimulate naturally fractured geothermal wells, and (iii) to determine the cause of reinjection problems (SM Benson & Bodvarsson, 1986).

A summary of early worldwide experience on the effects of cold water injection into geothermal reservoirs was presented by Horne (1982). His report included information from geothermal systems in New Zealand, Japan, El Salvador, and Philippines. It explained that these injection experiences could explain permeability changes, flow paths, and thermal and hydraulic connections with surrounding wells. Also in the same year, Grant (1982) discussed observed trends in injectivity and productivity for wells at Ngawha and Broadlands. He concluded that for these two systems, the fractured reservoir acts for injection in a very different manner than for production.

Kitao *et al.* (1990) discussed injection experiments conducted in three production wells in Sumikawa geothermal field. The results indicated that in most cases the injectivity of the wells was at least slightly improved. Ariki and Hatakeyama in 1998 carried out another injection experiment in well SD-1 at Sumikawa to evaluate the effect of water temperature on injectivity and found a similar result, namely, that reducing the injectate temperature increased the injectivity index and also reduced the apparent reservoir pressure at the feed zone.

Nakao and Ishido (1997) simulated data from injection experiments of Yatsubo-2 using DIAGNS and STAR (Pritchett, 1995), a general-purpose geothermal reservoir simulator. They suggested that injection has a strong influence on fracture opening. In addition, a skin effect was claimed to be necessary to produce the observed gradual pressure decline during fall-off. It was likewise noted that the increase in porosity and permeability experienced during the injection period diminished during the fall-off phase.

An in-depth numerical study was conducted by Ariki and Akibayashi (2001) to investigate the effects of injection temperature on the injection capacity of geothermal wells. They described the effects of several parameters such as injection location, fracture spacing, gravity and parameters in the Kozeny-Carman equation. Though comparison between measured and simulated values was not made, it was concluded that injection capacity is enhanced by injection of low temperature water.

A recent study by Wessling *et al.* (2009) analyzed downhole pressure measurements during hydromechanical stimulation. Their study used a simple reservoir model containing a single vertical fracture. Verga *et al.* (2011) employed a 2D axial symmetric model to simulate pressure behavior during injection tests and compared the results with those obtained using commercial software. A satisfactory simulation of the fall-off period was obtained.

The present study presents the results of utilizing TOUGH2 and FEHM to replicate the pressure transient data measured during injection tests on two geothermal wells. Inverse modeling was performed using PEST and iTOUGH to automatically determine best-fit model parameters and to analyse the sensitivity of the results to the values of the estimated parameters. The pressure transient data were also analyzed using commercial well testing software (SAPHIR and AWTAS) for further validation of the simulation results.

2. NUMERICAL SOFTWARE AND INVERSE MODELING

The numerical simulators TOUGH2 (Pruess, 1991) and FEHM (Zyvoloski, Dash, & Kelkar, 1988) were used for the thermal hydrological flow simulation while iTOUGH (Finsterle, 1998; Finsterle, Faybishenko, & Sonnenborg, 1998) and PEST (Doherty, 1994, 2005) were used for parameter optimization. AWTAS (O'Sullivan *et al.*, 2005) and SAPHIR (http://www.kappaeng.com/software/saphir), on the other hand were used for validation and comparison

of the simulated values. The description of the software given here is limited, but more complete documentation is available from the various websites.

TOUGH2 is a numerical simulator for non-isothermal flows of multi-component, multiphase fluids in porous and fractured media, developed at Lawrence Berkeley National Laboratory. It solves the basic conservation equations for mass, energy and momentum (through Darcy's law). The space discretization used by the numerical code is known as the integral finite difference (IFD) method. It is a well-established code used in many studies. It is the main simulation tool used in this study.

Aside from TOUGH2, the other numerical code used in this study is FEHM , which was developed at the Los Alamos National Laboratory. It also uses a discrete implementation of the conservation equations for mass, energy and momentum. The primary numerical method used in the code is the finite element method (Zienkiewicz, 1977; Zyvoloski, 1983, 2007) but a modification developed in 2007 also implements the finite volume method.

For parameter optimization, two approaches were used namely, iTOUGH and PEST. The first inverse modeling software used in this study was iTOUGH. This code was also developed at the Lawrence Berkeley National Laboratory and is designed specifically for use with the TOUGH2 family of codes. The iTOUGH code is capable of estimating TOUGH2 input parameters by calibrating the model against observed data. It also performs detailed residual calculations, error analysis and uncertainty estimation.

The software PEST was also used in this study. PEST stands for Parameter ESTimation and is a program with various utilities for parameter estimation and sensitivity analysis. It can be used with any simulator for the forward modeling runs and is applied here with TOUGH2 as well as with FEHM.

The parameter values calculated using the two optimization methods were compared with the values generated using commercial well test analysis software: AWTAS and SAPHIR. AWTAS is an automated well test analysis program with similar functionality to TOUGH2 in terms of modeling flows but uses fast numerical methods for solving the simple radial flow models that it uses. This program uses the same nonlinear regression techniques for parameter estimation that are used in codes such as AUTOMATE (Horne, 1995) and iTOUGH. Lastly, SAPHIR is pressure transient analysis software distributed by KAPPA Engineering. It is based on the analysis of the derivative of the pressure transient data. It provides ease of use and good graphical representations of results. In addition, it gives detailed reservoir characteristics.

3. WELL INJECTION TEST

Data were gathered and analyzed for injection tests that have been carried out on three types of geothermal wells: (i) newly drilled, (ii) have undergone a work-over or (iii) have experienced stimulation with acid injection or prolonged water injection.

Well A is a production well with a total measured depth of 3286m and is thought to have two permeable zones. Initial evaluation of the multi-rate pumping test shows that it has an injectivity of 9 l/s-MPa. However, positive wellhead pressure was observed during the maximum pump rate which could be a possible indication of low permeability. Because of this result a hydro-fracturing/prolonged water injection test was conducted.

After hydro-fracturing/extended cold water injection, another multi-rate pumping test was performed. Although no appreciable increase in the injectivity index was calculated, there was an average reduction of measured downhole pressure of about 2.4 MPa for each of the pump rates. In addition, there was a reduction of the calculated skin value.

Well B is another production well which was completed with a total depth of 2630m. A post-drilling multi-rate pumping test yielded an index of 8.2 l/s-MPA and indicated a distinct permeable zone at 2300 – 2400mMD. A number of attempts to discharge the well were made but were unsuccessful.

Re-entry activities for Well B were programmed in order to improve its productivity. Part of this set of activities was a baseline pressure-temperature-spinner (PTS) survey during an injection/fall-off test. The data collected from this survey is one of the sets used in this study. Deepening of the well was finished and reached a total depth of 3147mMD. Another injection test was performed to test for any improvement in performance of the well after deepening. These pressure response data are also used in this study.

4. NUMERICAL MODEL DESCRIPTION

The numerical models used in this study have a simple geometry. The well and the reservoir are represented by a single layer radially symmetric mesh with the well located along the axis of symmetry. Several authors such as Kazemi (1969) , Nakao and Ishido (1998), Verga *et al*. (2011), and Wessling *et al*. (2009) have used a similar model for their simulation studies. The model shown in Figure 1 was divided into different regions to represent the well and the reservoir materials. The wellbore where the fluid is injected has a radius of about 0.1m, which is a reasonable size compared to an actual casing of a well. The reservoir region was extended to a few thousand meters to eliminate boundary effects.

Most of the initial simulation results did not satisfactorily match the measured data and a stage-wise simulation only slightly improved the results.

In the next stage of modeling, it was decided to include the effect of a possible skin region, defined to measure the degree of damage or improvement of near well-bore permeability. This skin region was also specified during the simulation study of Nakao and Ishido (1998) on Yatsubo 2. Several other studies have focused on the significance of this region during the simulation process (S. Benson, 1982; SM Benson & Bodvarsson, 1986; SM Benson, Daggett, Iglesias, Arellano, & Ortiz-Ramirez, 1987; Nakao & Ishido, 1998; Verga et al., 2011). The numerical model used is shown in Figures 1.

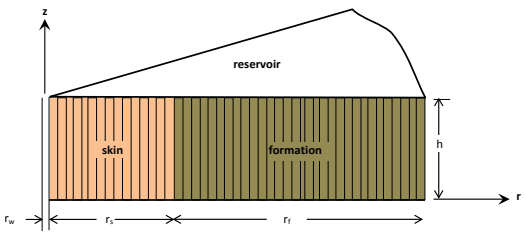

Figure 1: Reservoir model defining regions for the well, the skin zone and the reservoir

In the model, the skin radius was fixed while the other factors were allowed to vary. Different values of the skin radius were tested together with various permeability combinations. Both single porosity and dual porosity or MINC models (Pruess and Narasimhan, 1985) are investigated.

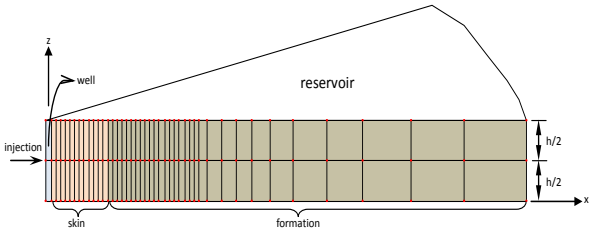

Figure 2: Reservoir model mesh in FEHM defining regions for the well, the skin and the reservoir

The grid used with FEHM, on the other hand, has differences due to the inherent mesh requirements. The model now consists of three layers of nodes, as shown in Figure 2. Similar to the model used in the TOUGH2 runs, it is divided into different regions that represent the well, the skin zone and the reservoir formation. The fluid was injected at the middle node in the column that represents the wellbore. For comparison with the FEHM model, a multilayered TOUGH2 model was also generated.

The initial temperature for all models is set at 200°C which is an appropriate value for the two wells considered

5. APPLICATION TO FIELD TEST DATA AND RESULTS.

The numerical models described in the preceding section were used to investigate the response of geothermal reservoirs to cold injection tests. Pressure transient data from two geothermal wells were analyzed using these models. The following nine approaches were used in this study:

Case 1 – TOUGH-PEST, Single Layer, 2 Materials (Well and Reservoir), Porous Media

Case 2 – TOUGH-PEST, Single Layer, 3 Materials (Well, Reservoir and Skin) Porous Media

Case 3 – TOUGH-iTOUGH, Single Layer, 2 Materials (Well and Reservoir), Porous Media

Case 4 – TOUGH-iTOUGH, Single Layer, 3 Materials (Well, Reservoir and Skin) Porous Media

Case 5 – TOUGH-PEST, Multi-Layer, 3 Materials (Well, Reservoir and Skin) Porous Media

Case 6 – FEHM-PEST, Multi-Layer, 2 Materials (Well and Reservoir), Porous Media

Case 7 – FEHM-PEST, Multi-Layer, 3 Materials (Well, Reservoir and Skin) Porous Media

Case 8 – TOUGH-PEST, Single Layer, 2 Materials (Well and Reservoir), MINC for Reservoir Material

Case 9 - TOUGH-PEST, Single Layer, 2 Materials (Well and Reservoir), Porous Media, Stage-wise

These various procedures were used to simulate the recorded pressure behavior and to achieve a best fit between simulated and measured values. Parameters such as porosity, permeability and compressibility of each material were optimized in each case. It was also observed that initial pressure of the reservoir affects the results and thus it was included in the list of parameters that were optimized.

These methods were first applied to the pressure transient data for Well A which were recorded after the well had undergone extended cold water injection/hydrofracturing. Calculated values for the parameters for Cases 1-4 are presented in Table 1. The values shown in Table 1 of the computed parameters from either PEST or iTOUGH are comparable except for the permeability of the skin material. It can also be noticed that the computed permeability for the reservoir is around 52 – 61 mD for a 2-material model with no skin region. This value is reduced to 11 – 26 mD when a skin region is added. The permeability of the skin on the other hand is about 5-10 times that of the reservoir permeability. The initial pressure computed is similar in all cases shown.

Table 1. Optimized parameters for Cases 1-4 of Well A

	Case 1	Case 2	Case 3	Case 4
Well				
Porosity, ϕ	1.0	0.975	1.0	1.0
Permeability, k	1.0 E-12	1.0 E-12	7.94 E-11	5.45 E-12
Compressibility, C	6.5 E-07	2.24 E-08	5.94 E-07	5.86 E-07
Reservoir				
Porosity, ϕ	0.025	0.01	0.01	0.01
Permeability, k	5.15 E-14	1.13 E-14	6.12E-14	2.64 E-14
Compressibility, C	1.00 E-08	1.50 E-10	1.00 E-10	5.496 E-10
Skin / Fracture				
Porosity, ϕ		0.11		0.037
Permeability, k		1.73 E-13		6.20 E-14
Compressibility, C		9.95 E-09		4.62 E-09
P_initial, MPa	16.84	16.41	16.99	16.70

The simulated pressure transients using the parameters in Table 1 are shown in Figure 3. The simulated pressure for the 2-material model exhibits a very sharp pressure fall-off. On the other hand the pressure simulated using the 3-material model adequately fits the fall-off data. The 3-material model developed using TOUGH-PEST shows a gradual decline in pressure during the fall-off phase whereas the same type of model developed with TOUGH-iTOUGH shows a rapid decline. The simulated pressures for the 3-material model are generally lower during injection, especially in the earlier stages, than for the 2-material model.

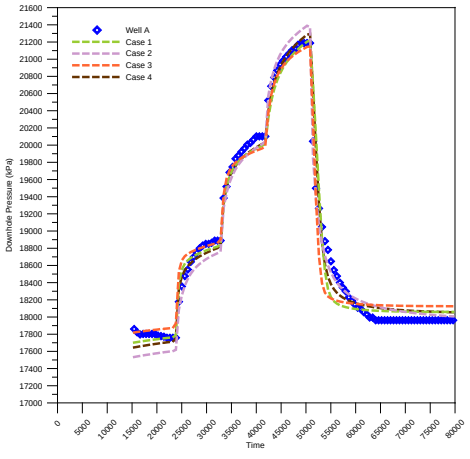

Figure 3: Simulated pressure response of Well A using parameter values from Table 1 for Cases 1-4

Table 2 gives the results of parameter optimization for Cases 5-7. These are the multilayer models using both TOUGH-

PEST and FEHM-PEST combinations. The multilayer TOUGH-PEST reservoir parameters are almost the same as for the single layer TOUGH-PEST case. However, the FEHM-PEST model yields a very different result. The 2-material model FEHM-PEST produced a permeability of 164 mD compared to 52 – 61 mD for the 2-material model for TOUGH-PEST or TOUGH-iTOUGH.

Table 2: Optimized parameters for Cases 5-7, Well A

	Case 5	Case 6	Case 7
Well			
Porosity, ϕ	1.0	1.0	0.9
Permeability, k	1.0 E-11	1.0 E-11	1.0 E-10
Compressibility, C	5.025 E-07		
Reservoir			
Porosity, ϕ	0.107	0.2	0.05
Permeability, k	1.64 E-14	1.64 E-13	9.23 E-15
Compressibility, C	1.00 E-10		
Skin / Fracture			
Porosity, ϕ	0.2		0.2
Permeability, k	1.0 E-12		1.0 E-12
Compressibility, C	1.00 E-08		
P_initial, MPa	16.627	17.092	16.504

However, for FEHM-PEST (Case 7), the permeability value for the reservoir (~ 9mD) is comparable to the value from Case 2 but only half that of Case 4. The value of the initial pressure for Cases 5 and 7 are almost the same but the value for Case 6 is a little higher.

Figure 4 shows plots of the simulated pressures for Cases 5-7. It can also be seen that the pressure transient plot for the 2-material FEHM-PEST model (Case 6) shows a sharp pressure rise and fall at a change of injection rate. However, Cases 5 and 7 show good matches between model and measured values for the whole duration of the test, including the gradual change in the pressure during fall-off.

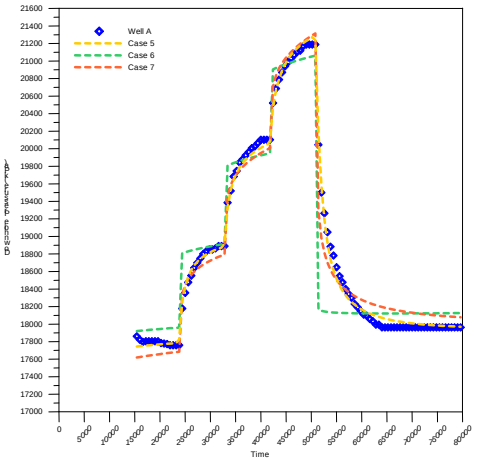

Figure 4: Simulated pressure transient response of Well A using parameter values from Table 2, Cases 5-7

The second set of data examined is the pressure transient recorded during the injection tests on Well B. The first test was conducted after the well was drilled and attempts to discharge it had been made. This data set will be denoted as Well B-1 to distinguish it from another set of data from the same well which was recorded after the well was deepened (called here Well B-2).

Table 3 presents the results for Cases 1-4 for Well B-1. The values of the formation permeability range from 6 – 71 mD. Both optimization methods yield consistent results. The 2-material models have a 10 times higher reservoir permeability than that for the 3-material models.

The initial pressure value calculated from the two optimization procedures is almost the same for corresponding model types although there is a difference of about 0.7 MPa between the values for the 2-material and 3-material models.

Table 3: Optimized parameters for Cases 1-4, Well B-1

	Case 1	Case 2	Case 3	Case 4
Well				
Porosity, ϕ	1.00	0.900	1.00	.9000
Permeability, k	1.00 E-11	1.93 E-12	1.00 E-10	9.88 E-11
Compressibility, C	4.930 E-07	1.417 E-08	4.759 E-07	1.646 E-08
Reservoir				
Porosity, ϕ	0.20	0.198	0.20	.01230
Permeability, k	7.16 E-14	6.24 E-15	7.12 E-14	8.113E-15
Compressibility, C	1.00 E-08	2.311 E-09	1.000 E-08	1.944E-09
Skin / Fractured				
Porosity, ϕ		0.059		.0518
Permeability, k		3.33 E-13		1.72 E-13
Compressibility, C		1.451 E-09		2.753E-09
P_initial, MPa	11.533	10.270	11.573	10.382

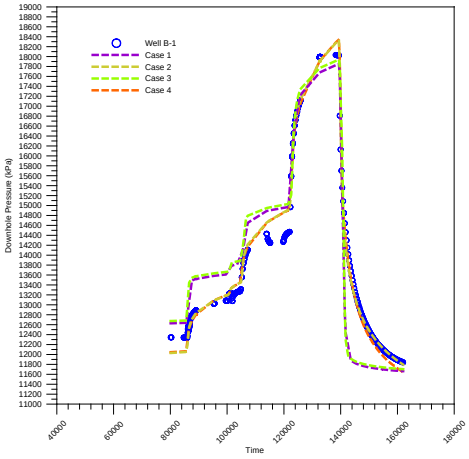

Figure 5: Simulated pressure response of Well B-1 using parameter values from Table 3 for Cases 1-4

The resulting values shown in Table 3 were used to simulate the pressure transient for Well B-1 shown in Figure 5. The figure shows that Cases 1 and 3 did not yield a satisfactory match to either the injection or fall-off stages. For both cases there is a sharp drop in pressure during the fall-off. On the other hand, Cases 2 and 4 both show an acceptable match to the measured data, especially the gradual drop in pressure during fall-off. Some of the details of the pressure response are not matched well.

The parameters from the simulations for Cases 5-7 are given in Table 4. The parameters shown in this table for the multilayer TOUGH-PEST run are similar to those for the single layer TOUGH PEST run, as was previously observed to be the case for Well A. Although the reservoir permeability values computed for Case 5 and Case 7 are similar, about 10.8 mD compared to 13.8 mD, the permeability value for Case 6 is an order of magnitude higher. The computed initial pressure varied for these cases, ranging from 10.5 MPa to 12.2 MPa.

Figure 6 shows the simulated pressure transient response for Cases 5-7 using the parameter values in Table 4. As for Well A, Case 6 did not produce a good match between the measured and the simulated values. It also showed a sudden

pressure drop during the fall-off stage. Cases 5 and 7 for Well B-1 also produce a good fit for most of the stages, especially the fall-off phase.

Table 4: Optimized parameters for Cases 5-7 of Well B-1

	Case 5	Case 6	Case 7
Well			
Porosity, ϕ	0.90	1.00	1.00
Permeability, k	1.25 E-12	1.00 E-11	1.00 E-10
Compressibility, C	1.756 E-10		
Reservoir			
Porosity, ϕ	0.20	0.20	0.20
Permeability, k	1.38 E-14	2.26 E-13	1.08 E-14
Compressibility, C	1.000 E-08		
Skin / Fractured			
Porosity, ϕ	0.200		0.20
Permeability, k	1.16 E-12		1.00 E-12
Compressibility, C	1.000 E-10		
P_initial, MPa	10.574	12.179	11.211

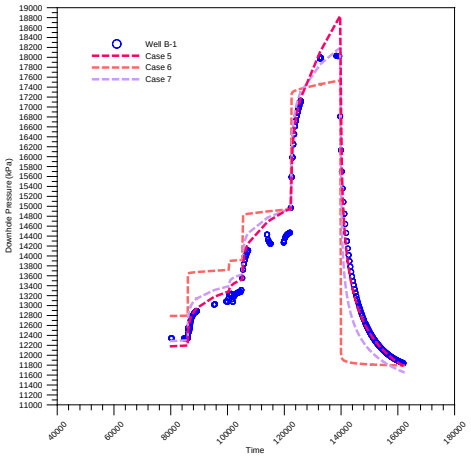

Figure 6: Simulated pressure transient response of Well B-1. Parameter values from Table 4, Cases 5-7

After exploring models based on a single porosity, porous medium, a dual porosity MINC model was also set up. The resulting parameters for this model are given in Table 5. This table shows that for Well A the matrix should have a permeability of 0.84mD and a fracture permeability of around 74mD. On the other hand, the matrix permeability is 10mD and a fracture permeability of 77mD for Well B. The values presented in this table are comparable to the values in Tables 1 and 3.

Table 5. Optimized parameters for the dual porosity model (Case 8) for Wells A and B-1

Case 8	Well A	Well B-1
Well		
Porosity, ϕ	0.95	1.00
Permeability, k	1.96 E-12	9.99 E-12
Compressibility, C	1.055 E-08	5.226 E-07
Reservoir		
Porosity, ϕ	0.12	0.20
Permeability, k	8.41 E-16	1.00 E-14
Compressibility, C	1.000 E-09	1.000E-07
Skin / Fracture		
Porosity, ϕ	0.82	0.80
Permeability, k	7.41 E-14	7.76 E-14
Compressibility, C	1.191 E-09	1.531 E-10
P_initial, MPa	17.171	11.462

The pressure transient behavior for Case 8 for Wells A and B-1 using the parameters in Table 5 are shown in Figures 7a and 7b for each well. The results are presented together with those for Cases 1 and 2 for comparison. It can be seen that for both wells, the use of a MINC model to simulate the pressure responses did not much improve the fit to the data and the results are quite similar to the ones generated for Case 1. Case 2 which includes a "skin" layer yielded a more satisfactory result.

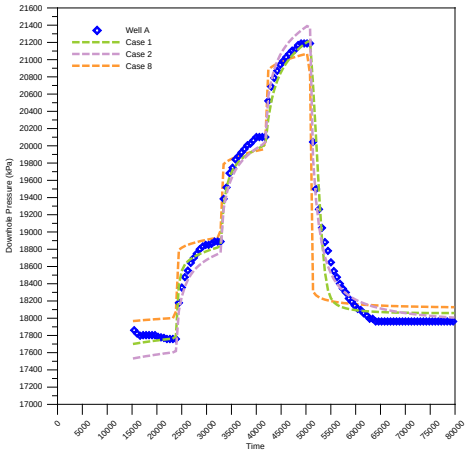

Figure 7a. Comparison of the simulated pressure response of Well A for Cases 1, 2, and 8

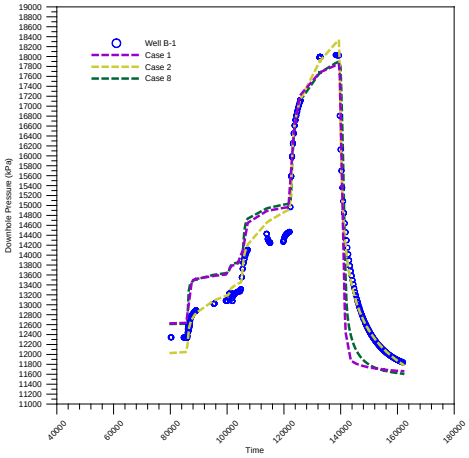

Figure 7b. Comparison of simulated pressure transient response of Well B-1 for Cases 1, 2, and 8

A pressure transient data set (called Well B-2 here) was examined for another injection test conducted at Well B. This data was collected after the well was deepened during the re-entry activity mentioned earlier. The best-fit parameters for Cases 1-4 for this set of data are presented in Table 6. This table shows that the estimated reservoir permeability ranges from 14mD to 106 mD. The values for the reservoir permeability for Cases 1 and 3 are similar in magnitude while the permeability value estimated for Case 4 is about four times that for Case 2. The calculated skin permeability for Case 2 is seven times greater than that computed with Case 4. The initial pressure estimated is variable, ranging from 12.405 MPa to 13.174 MPa.

Figure 8 presents the pressure transient data simulated using the parameter values given in Table 6. Most of the plots fit best during the early stages of injection. It should also be noted that there is a sharp pressure decline during fall-off for Cases 1 and 3. This is not the situation for Cases 2 and 4 although it is apparent that Case 2 yields a better match to the data. Unfortunately, the matches for Well B-2 are

generally poor compared to the results generated for the other well data.

Table 6. Optimized parameters for Cases 1-4, Well B-2

	Case 1	Case 2	Case 3	Case 4
Well				
Porosity, ϕ	0.90	1.00	1.00	1.00
Permeability, k	1.00 E-11	1.00 E-12	1.00 E-10	1.00 E-10
Compressibility, C	7.523 E-08	3.464 E-08	1.206 E-07	3.061 E-10
Reservoir				
Porosity, ϕ	0.20	0.074	.20	0.01
Permeability, k	1.05 E-13	1.38 E-14	1.06 E-13	6.56 E-14
Compressibility, C	1.000 E-08	1.962 E-10	1.000 E-08	1.943 E-10
Skin / Fractured				
Porosity, ϕ		0.20		.347
Permeability, k		7.33 E-13		1.14 E-13
Compressibility, C		1.000 E-08		1.000 E-08
P_initial, MPa	13.152	12.405	13.174	12.861

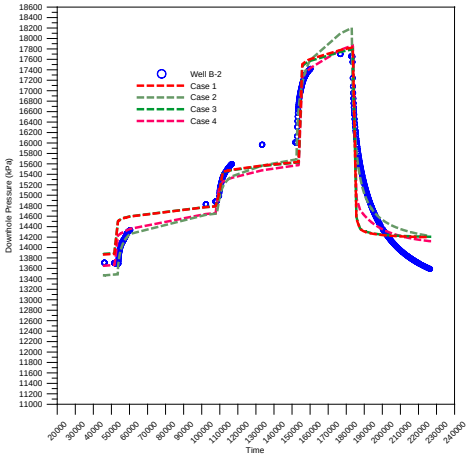

Figure 8. Simulated pressure response of Well B-2 using parameter values from Table 6 for Cases 1-4

Parameters for Cases 5 to 7 for Well B-2 are given in Table 7. The permeability values for Cases 5 and 7 vary between 19.6mD to 46mD which is within the range mentioned for Cases 1 to 4. The initial pressures presented in Table 7 are similar to the ones presented for Cases 2 and 4 in Table 6. The permeability of the skin is at least twice that of the reservoir. As encountered earlier, the permeability of the reservoir for Case 6 is an order of magnitude higher than for Cases 5 and 7.

Table 7. Optimized parameters for Cases 5-7 of Well B-2

	Case 5	Case 6	Case 7
Well			
Porosity, ϕ	1.00	1.00	1.00
Permeability, k	1.90 E-12	1.00 E-11	1.00 E-10
Compressibility, C	7.790 E-07		
Reservoir			
Porosity, ϕ	0.20	0.20	0.20
Permeability, k	4.60 E-14	3.75 E-13	1.96E-14
Compressibility, C	2.355 E-09		
Skin / Fractured			
Porosity, ϕ	0.20		0.20
Permeability, k	6.25 E-13		1.00 E-12
Compressibility, C	1.000 E-08		
P_initial, MPa	12.809	13.542	12.607

The resulting transient plots based on the parameter values in Table 7 are shown in Figure 9. It is evident from this figure that Case 6 does not yield a good fit to the data and has sharp pressure changes following an increase or decrease of the pump rate. The fall-off results for Cases 5 and 7 do not exhibit the distinct gradual change in pressure during the fall-off stage but the curves generated from these cases have a gentle slope compared to that for Case 6.

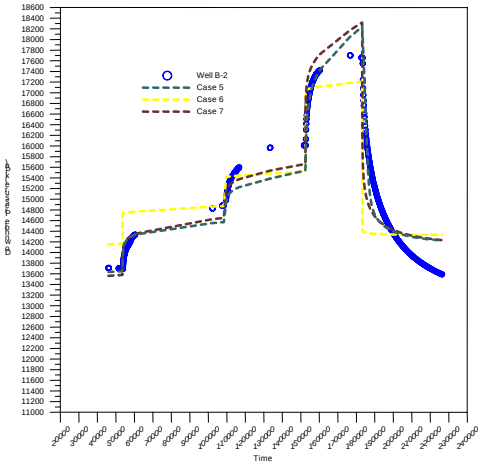

Figure 9. Simulated pressure response of Well B-2, using parameter values from Table 7, Cases 5-7

The simulations for the cases discussed so far involve a single simulation run and a single set of parameters for the injection-fall-off phase. Since the model does not fit acceptably throughout the pressure transient response for each well data, the possibility that the reservoir parameters vary from stage to stage of the test was also investigated. A stage-wise simulation for this purpose was carried out and will be the identified as Case 9. The parameters resulting for this case are presented in Table 8 and are quite interesting. For Wells A and B-2 the permeability increases considerably during injection. However, the permeability diminishes again during the fall-off stage. This is also observed from the simulation of Well B-1.

The graphs presented in Figures 10a-c show the pressure transient behavior simulated using the parameter values given in Table 8. It is evident that very good matches were obtained for the injection stage however; the fall-off phase again shows a sudden pressure drop, which was also encountered in earlier cases especially those not using a skin zone.

Table 8. Optimized parameters for Case 9, Wells A, B-1, and B-2

Case 9	Well A	Well B-1	Well B-2
Well			
Porosity, ϕ	1.00	0.96	1.00
Permeability, k	1.00 E-12	4.26 E-12	2.67 E-12
Reservoir			
Stage 1-4 Porosity, ϕ	0.076	0.20	0.20
Stage 1 Permeability, k	2.62 E-14	6.68 E-14	2.05 E-14
Stage 2 Permeability, k	3.62 E-14	8.63 E-14	3.56 E-14
Stage 3 Permeability, k	4.03 E-14	7.72 E-14	4.42 E-14
Stage 4 Permeability, k	4.53 E-14	6.91 E-14	6.54 E-14
Stage 5 Permeability, k	3.20 E-14	1.45 E-14	2.69 E-14
Stage 5 Porosity, ϕ	0.036	0.20	0.01
P_initial, MPa	16.000	11.060	10.000

5. COMPARISON WITH AWTAS AND SAPHIR

All sets of data for Well A and Well B used for Cases 1-9 were also analyzed using the well testing software SAPHIR and AWTAS. Although these software packages offer

numerous models, variation of reservoir type and boundary conditions, the study only considered models with a vertical well in a homogenous reservoir with an infinite boundary. The resulting parameters are given in Table 9 and Table 10 for SAPHIR and AWTAS, respectively.

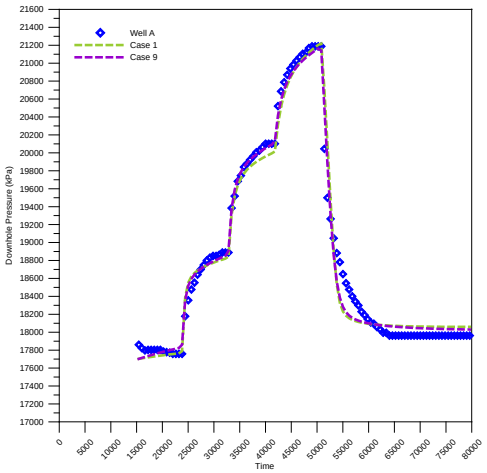

Figure 10a. Comparison of simulated pressure transient response of Well A for Cases 1 and 9

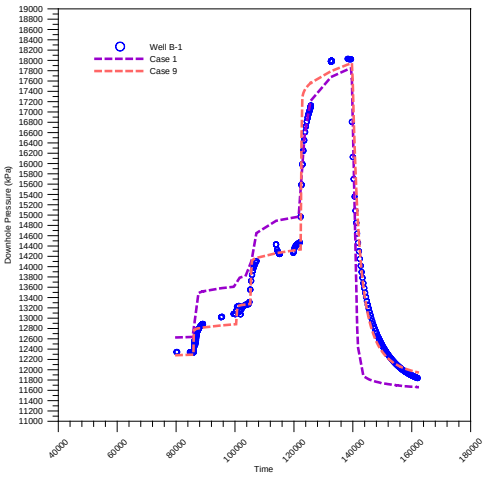

Figure 10b. Comparison of simulated pressure transient response of Well B-1 for Cases 1 and 9

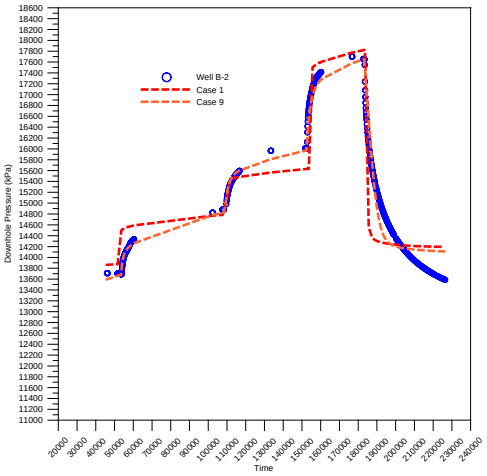

Figure 10c. Comparison of simulated pressure response of Well B-2 for Cases 1 and 9

The results presented in Table 9 for SAPHIR agree with the results for the cases above that include a skin zone. In addition, the permeability computed for Case 9 covers the permeability range shown with these results. The AWTAS results show a similar trend to the SAPHIR results although they are numerically slightly different.

Table 9. SAPHIR well test analysis results

SAPHIR	Well A	Well B-1	Well B-2
Permeability, k (mD)	31.3	8.44	35.2
Storage, C (m^3/kPa)	0.0202	0.0104	0.0552
Total Skin, S	2.61	-5.13	-0.7

Table 10. AWTAS well test analysis results

AWTAS	Well A	Well B-1	Well B-2
Permeability, k (mD)	25.2	12.8	21.2
Porosity, ϕ	0.01	0.02	0.027
Total Skin, S	-2.10	-3.74	-3.91

6. DISCUSSION AND CONCLUSIONS

Simulations were performed to model the pressure transient response of geothermal wells during injection tests, particularly to determine how the reservoir parameters vary. It was observed that for most cases where the model reservoir is made up of only one material (either porous or fractured media) with a single set of parameters, the pressure changes rapidly following an increase or decrease in the pump rate. In addition, the model results show a poor match to all stages of the test data.

The introduction of another material to represent the skin region improved the match, particularly the gradual decline in pressure during the fall-off period. This is a similar conclusion to the results published by Nakao and Ishido on their analysis of the Yatsubo 2 well data. However, it should be noted that the presence of the skin region gives lower pressure values during the injection stages especially on the initial pressure value of the reservoir. Based on these observations, it could be inferred that the skin region may not be present at the onset of injection.

Another interesting trend was established by the stage-wise simulation. It was observed that the permeability generally increases as the pump rate is increased. This effect has been previously noted by several authors e.g. Kitao et al., Benson, Ariki and Akibayashi, Contreras (1990), and Cox and Bodvarsson (1985).

However, the permeability seems to diminish during the fall-off phase of the tests. This might explain why some wells do not have a productivity as large as the injectivity.

It is worth mentioning that the fall-off stage was not satisfactorily matched using a model with a single reservoir material for any of the tests considered. This means that introducing a skin region in the model is useful. With a model that includes a skin region the increase in permeability gained during the injection may not be totally lost but could be retained in the finite skin zone near the well.

The results from the simulation using TOUGH and FEHM are consistent with the results obtained using the well test analysis software AWTAS and SAPHIR. This agreement validates the use of the methods discussed in this study for analysing other injection tests of geothermal wells.

The results of this study show that an injection test conducted on a geothermal well has an effect on reservoir permeability, with an apparent increase in permeability with each increase in injection rate. However, it appears that the permeability gained during injection diminishes again during the fall-off phase. It also seems that a skin region dictates the shape of the pressure transient during the early stages of the fall-off.

ACKNOWLEDGEMENT

The authors would like to thank Energy Development Corporation (EDC) for permission to use field data analyzed in this study. They would also like to acknowledge the help with this study of John Doherty, George Zyvoloski, and colleagues from EDC and University of Auckland.

REFERENCES

Ariki, K., & Akibayashi, S. (2001). Effects of the Injection Temperature on Injection-Capacity of Geothermal Wells-Numerical Study. *Geothermal Resources Council Transactions, 25*, 445-454.

Ariki, K., & Hatakeyama, K. (1998). Effects of Injection Temperature on the Injectivity of a Geothermal Well. *Geothermal Resource Council Transactions, 22*, 539-546.

Benson, S. (1982). *Interpretation of nonisothermal step-rate injection tests.* Paper presented at the Eight Workshop Geothermal Reservoir Engineering, Stanford University, Stanford, California.

Benson, S., & Bodvarsson, G. (1986). Nonisothermal effects during injection and falloff tests. *SPE Formation Evaluation, 1*(1), 53-63.

Benson, S., Daggett, J., Iglesias, E., Arellano, V., & Ortiz-Ramirez, J. (1987). *Analysis of thermally induced permeability enhancement in geothermal injection wells.* Paper presented at the 12th Workshop on Geothermal Reservoir Engineering, Stanford University, Stanford, California, 20-22 January 1987.

Contreras, E. A. (1990). Permeability changes during the flow of distilled water and brine through geothermal sandstones at temperatures of 25degC - 270degC. *Geothermal Resources Council transactions, 14*, 1183 - 1192.

Cox, B. L., & Bodvarsson, G. S. (1985). *Nonisothermal injection tests in fractured reservoirs.* Paper presented at the 10th Annual Workshop on Geothermal Reservoir Engineering, Stanford University, California, 22-24 January.

Doherty, J. (1994). PEST: a unique computer program for model-independent parameter optimisation. *Water Down Under 94: Groundwater/Surface Hydrology Common Interest Papers; Preprints of Papers*, 551.

Doherty, J. (2005). PEST Model-Independent Parameter Estimation User Manual: Watermark Numerical Computing.

Finsterle, S. (1998). *Multiphase inverse modeling: An overview.* Paper presented at the Geothermal Program Review XVI, Berkeley, California, April 1-2, 1998.

Finsterle, S., Faybishenko, B., & Sonnenborg, T. O. (1998). *Inverse modeling of a multistep outflow experiment for determining hysteretic hydraulic properties.* Paper presented at the TOUGH Workshop, Lawrence Berkeley National Laboratory, Berkeley, California, May 4-6.

Grant, M. A. (1982). *Measurement of permeability by injection tests.* Paper presented at the Eighth Workshop Geothermal Reservoir Engineering, Stanford University, Stanford, California.

Horne, R. (1982). *Effects of Water Injection into Fractured Geothermal Reservoirs: A Summary of Experience Worldwide*: Stanford Geothermal Program, Interdisciplinary Research in Engineering and Earth Sciences, Stanfor University, Stanford, California. *SGP-TR-57*

Horne, R. (1995). *Modern well test analysis: a computer aided approach* (2nd ed.): Petroway Inc. Palo Alto, California.

Kazemi, H. (1969). Pressure Transient Analysis of Naturally Fractured Reservoirs with Uniform Fracture Distribution. *Old SPE Journal, 9*(4), 451-462.

Kitao, K., Ariki, K., Hatakeyama, K., & Wakita, K. (1990). Well stimulation using cold-water injection experiments in the Sumikawa geothermal field, Akita prefecture, Japan. *Geothermal Resource Council Transactions, 14*, 1219–1224.

Nakao, S., & Ishido, T. (1998). Pressure-transient behavior during cold water injection into geothermal wells. *Geothermics, 27*(4), 401-413.

O'Sullivan, M. J., Croucher, A. E., Anderson, E. B., Kikuchi, T., & Nakagome, O. (2005). An automated well-test analysis system (AWTAS). *Geothermics, 34*(1), 3-25.

Pritchett, J. (1995). STAR User's Manual. *Report No. SSS-TR-92-13366*: S-Cubed, La Jolla, California.

Pruess, K. (1991). TOUGH2: A general-purpose numerical simulator for multiphase fluid and heat flow (pp. 102): Lawrence Berkeley National Laboratory, Berkeley, California.

Pruess, K., & Narasimhan, T. N. (1985). A Practical Method for Modeling Fluid and Heat Flow in Fractured Porous Media. *Society of Petroleum Engineer Journal, United States, 25*(1).

Verga, F., Viberti, D., & Borello, E. (2011). A new insight for reliable interpretation and design of injection tests. *Journal of Petroleum Science and Engineering, 78*(1), 166-177.

Wessling, S., Junker, R., Rutqvist, J., Silin, D., Sulzbacher, H., Tischner, T., & Tsang, C.-F. (2009). Pressure analysis of the hydromechanical fracture behaviour in stimulated tight sedimentary geothermal reservoirs. *Geothermics, 38*(2), 211-226.

Zienkiewicz, O. C. (1977). *The Finite Element Method*: McGraw-Hill, London.

Zyvoloski, G. (1983). Finite element methods for geothermal reservoir simulation. *International Journal for Numerical and Analytical Methods in Geomechanics, 7*(1), 75-86.

Zyvoloski, G. (2007). FEHM: A control volume finite element code for simulating subsurface multi-phase multi-fluid heat and mass transfer. *Los Alamos Unclassified Report LA-UR-07-3359*.

Zyvoloski, G., Dash, Z., & Kelkar, S. (1988). *FEHM: finite element heat and mass transfer code* (pp. 57). Los Alamos National Laboratory, Los Alamos, Mexico. *LA-11224-MS*